

# Lattice modes and free-carrier response of $\text{Al}_x\text{Ga}_{1-x}\text{N}$ and $\text{In}_x\text{Ga}_{1-x}\text{N}$ heterostructures and strained GaN-AIN-superlattices measured by infrared ellipsometry W 33086

M. Schubert\* T.E. Tiwald, and J. A. Woollam

A. Kasic and B. Rheinländer

J. Off, B. Kuhn and F. Scholz

S. Einfeldt and D. Hommel

\*email: schubert@engrs.unl.edu



University Nebraska-Lincoln, Center for Microelectronic and Optical Materials Research, NE 68588-0511 Lincoln, USA

Universität Leipzig, Fakultät für Physik und Geowissenschaften, Abteilung Halbleiterphysik, D-04103 Leipzig, Germany

Universität Stuttgart, 4. Physikalisches Institut, Kristalllabor, D-70550 Stuttgart, Germany

Universität Bremen, Institut für Festkörperoptik, D-28359 Bremen, Germany

Research supported in part by Deutsche Forschungsgemeinschaft Project Rh 28/3-1 (Germany), and in part by NSF contract DMI-9901510 (USA)

## Outline

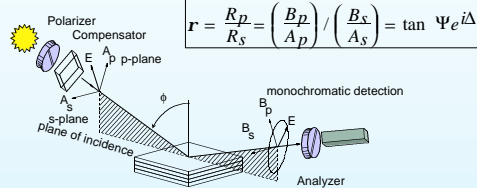
We determine the anisotropic dielectric functions of wurtzite III-N materials grown by MOCVD or MBE on (0001) sapphire using spectroscopic ellipsometry (SE) within the infrared (IR) spectral range [ 333  $\text{cm}^{-1}$  (30  $\mu\text{m}$ ) ... 3333  $\text{cm}^{-1}$  (3  $\mu\text{m}$ )].

We present phonon-mode frequencies and free-carrier parameters in:

- Si-doped *n*-type and Mg-doped *p*-type *a*-GaN
- *a*- $\text{Al}_x\text{Ga}_{1-x}\text{N}$  ( $0 < x < 1$ ) and *a*- $\text{In}_x\text{Ga}_{1-x}\text{N}$  ( $x < 0.3$ )
- strained GaN-AIN superlattice structure.

We discuss energy-dependence of electron and hole effective mass in *a*-GaN, and strain in *a*-GaN-AIN-SL structure.

## Spectroscopic ellipsometry (SE)



$$r = \frac{R_p}{R_s} = \left( \frac{B_p}{A_p} \right) / \left( \frac{B_s}{A_s} \right) = \tan \Psi e^{i\Delta}$$

Ellipsometry measures the ratio of  $R_p$  vs.  $R_s$  [Azzam-89] in terms of  $\Psi$  and  $\Delta$ . Model calculations are performed until measured and calculated data match as closely as possible [Jellison-98]. The mean-square error function employed is weighted to the experimental errors [Herzinger-95].

## III-Nitride dielectric function model

A factorized model [Gervais-74] is employed for the lattice contribution. The Drude approximation is used to calculate the free-carrier response [Wolfe-89]. LO, TO phonons, and broadening parameters:  $\omega_{LO}$ ,  $\omega_{TO}$ ,  $g_{LO}$ ,  $g_{TO}$ . Polarization perpendicular to the *c*-axis: ( $E_{\perp}$ )-modes. Polarization parallel to the *c*-axis: ( $A_{\parallel}$ )-modes. See, e.g., [Orton-98].

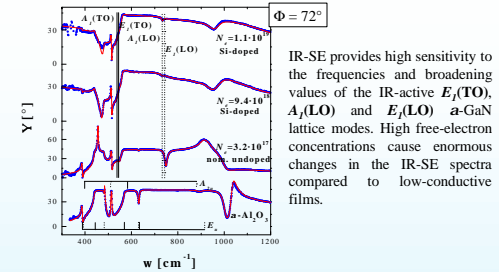


$$\epsilon_{\perp} = \epsilon_{\infty} \prod_j \frac{\omega_{LOj}^2 - \omega^2 - i\omega g_{LOj}}{\omega_{TOj}^2 - \omega^2 - i\omega g_{TOj}} + i \frac{e^2 n}{m_j \omega} \left( \frac{t_{mj}}{\tau_j} \right)_{j=\perp}$$

The effective mass  $m_j^*$  and the energy-averaged carrier momentum life time  $\langle t_{mj}^* \rangle$  are anisotropic.  $\langle t_{mj}^* \rangle$  is substituted by the optical carrier mobility  $\mu_j$ .

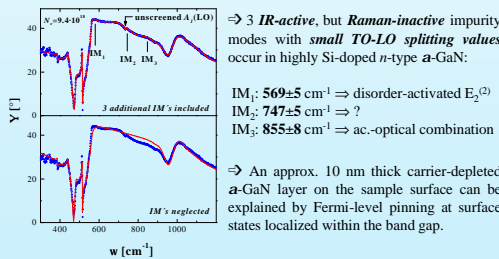
$$\left( \frac{t_{mj}}{\tau_j} \right)_{j=\perp} = \left( \frac{t_{mj}}{\tau_j} (1 - i\omega t_{mj}) \right)_{j=\perp} \Rightarrow \left( \frac{t_{mj}}{\tau_j} \right)_{j=\perp} = \left( \frac{m_j^*}{m_0} \right)_{j=\perp} \mu_j$$

## *n*-type *a*-GaN/*a*- $\text{Al}_2\text{O}_3$



IR-SE provides high sensitivity to the frequencies and broadening values of the IR-active  $E_1(\text{TO})$ ,  $A_1(\text{LO})$  and  $E_1(\text{LO})$  *a*-GaN lattice modes. High free-electron concentrations cause enormous changes in the IR-SE spectra compared to low-conductive films.

## Impurity modes & depletion layer



$\Rightarrow$  3 IR-active, but Raman-inactive impurity modes with small TO-LO splitting values occur in highly Si-doped *n*-type *a*-GaN:

- IM<sub>1</sub>: 569 ± 5  $\text{cm}^{-1} \Rightarrow$  disorder-activated  $E_2^{(2)}$
- IM<sub>2</sub>: 747 ± 5  $\text{cm}^{-1} \Rightarrow ?$
- IM<sub>3</sub>: 855 ± 8  $\text{cm}^{-1} \Rightarrow$  ac.-optical combination

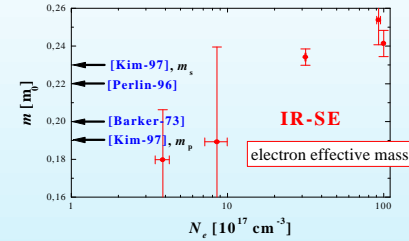
$\Rightarrow$  An approx. 10 nm thick carrier-depleted *a*-GaN layer on the sample surface can be explained by Fermi-level pinning at surface states localized within the band gap.

## Electron and hole effective mass in *a*-GaN

By performing the model based IR-SE data analysis we determine the anisotropic

- phonon frequencies and broadening values ( $\Rightarrow$  layer strain and quality),
- dielectric function,
- high-frequency dielectric constant,
- the free-carrier parameter values (effective mass and carrier mobility), and the layer thickness of the *a*-GaN layers.

Especially in the case of Si-doped *n*-type *a*-GaN we find a dependence of the (isotropically averaged) effective mass on the carrier concentration using the carrier Hall mobility as input parameter for our model calculations.

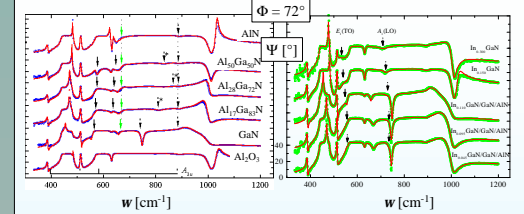


Because of small hole concentration ( $N_h \leq 3 \cdot 10^{18} \text{ cm}^{-3}$ ) and typical strong plasmon damping in *p*-type *a*-GaN, the determination of the free-hole parameter values is difficult. Nevertheless, IR-SE provides the hole mobility values as well as the hole effective mass  $m_h$  without substantial anisotropy.

$N_h [\text{cm}^{-3}]$	$m_h [m_0]$	hole effective mass
$5 \cdot 10^{17}$	$0.74 \pm 0.17$	
$8 \cdot 10^{17}$	$1.40 \pm 0.33$	

## *a*- $\text{Al}_x\text{Ga}_{1-x}\text{N}$

## *a*- $\text{In}_x\text{Ga}_{1-x}\text{N}$



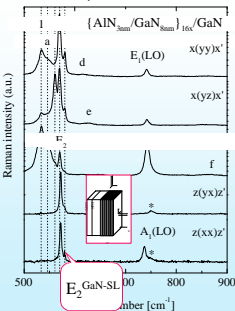
IRSE ( $\Psi$ ) data for *a*- $\text{Al}_x\text{Ga}_{1-x}\text{N}$  and *a*- $\text{In}_x\text{Ga}_{1-x}\text{N}$  heterostructures grown on *a*- $\text{Al}_2\text{O}_3$ . The sapphire reststrahlen bands ( $A_{2u}$ ,  $E_u$ ) are present throughout all spectra, and those of a bare (0001) substrate are included for comparison (See Ref. [Schubert-PRB-00]). The *a*- $\text{Al}_x\text{Ga}_{1-x}\text{N}$  spectra shown here reveal a two-(one) mode behavior for  $E_{\perp c}$  ( $E_{\parallel c}$ ), and are influenced by free carriers (See Ref. [Schubert-MRS-99]). The *a*- $\text{In}_x\text{Ga}_{1-x}\text{N}$  spectra reveal a single mode behavior.

*a*-III-N phonon modes determined so far by IR-SE. For *a*- $\text{Al}_x\text{Ga}_{1-x}\text{N}$  two IR-active  $E_{\perp}$ -modes are present for  $0 < x < 1$ .

TABLE I: *a*- $\text{Al}_x\text{Ga}_{1-x}\text{N}$  "impurity" modes ( $x \rightarrow 0, 1$ )

Impurity Mode	substrate	method	$\omega(\text{GaN } E_{\perp})$ ( $x \rightarrow 1$ ) [ $\text{cm}^{-1}$ ]	$\omega(\text{AlN } E_{\perp})$ ( $x \rightarrow 0$ ) [ $\text{cm}^{-1}$ ]
[Schubert-MRS-99]	$\text{Al}_2\text{O}_3$	IR-ellipsometry	605	638
[Wisniewski-98]	6H-SiC	IR-reflectometry	622	643

## $\mu$ -Raman

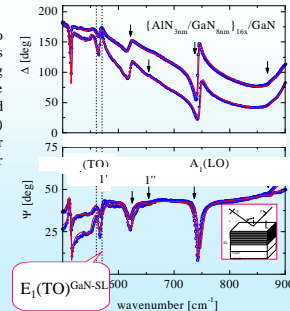


IR-SE ( $\Psi$ ) data and  $\mu$ -Raman spectra reveal additional SL-phonon modes similar to those observed in Ref. [Gleize-99]. The shift of the GaN-SL  $E_2$  and  $E_1(\text{TO})$  modes can be used to estimate the strain in the SL ([Davydov-97], [Tripathy-99]). Using elastic constants for GaN, the obtained stress ( $\sigma_{xx} \sim -4.5$  GPa) is very similar to the strain induced by the SL-sublayers if a common in-plane lattice constant is adopted within the SL structure ( $\sigma_{xx} \sim -3.15$  GPa). Furthermore, free-carriers ( $N_c \sim 8 \cdot 10^{18} \text{ cm}^{-3}$ ) with assumed effective mass  $0.22 \cdot m_0$  are located within the GaN-sublayers. Their vertical ( $\sim 32 \text{ cm}^2/(\text{Vs})$ ) and lateral ( $\sim 320 \text{ cm}^2/(\text{Vs})$ ) mobility values differ by a factor of 10!

## GaN-AIN-Superlattice

- GaN-sublayer:  $N_c \sim 8 \cdot 10^{18} \text{ cm}^{-3}$
- $m_e \sim 10 \cdot m_0 \Rightarrow 320 \text{ cm}^2/(\text{Vs})$
- $\Rightarrow$  vertical carrier confinement
- SL-biaxial stress:  $\sigma_{xx} \sim -4.5$  GPa
- $\Rightarrow$  strained GaN-AIN-SL

## IRSE



## Conclusions

IR-SE is an excellent tool to determine lattice phonon mode frequencies and free-carrier parameters in III-N thin films.

### References:

[Azzam-89] R. M. A. Azzam and S. M. Bahara, *Ellipsometry and Polarized Light* (North-Holland, Amsterdam, 1989).

[Jellison-98] G. E. Jellison, *Thin Solid Films*, 313-314, 33 (1998).

[Herzinger-95] C. M. Herzinger et al., *J. Appl. Phys.* 77, 1715 (1995).

[Gervais-74] F. Gervais and B. Piron, *J. Phys. C*, 7, 2574 (1974).

[Wolfe-89] C. M. Wolfe, N. Holonyak, G.E. Stillman, *Physical Properties of Semiconductors* (Prentice Hall, New Jersey, 1989).

[Orton-98] J. W. Orton and C. T. Foxon, *Rep. on Prog. Phys.* 61, 1 (1998).

[Wisniewski-98] P. Wisniewski et al., *Appl. Phys. Lett.* 73, 1760 (1998).

[Schubert-MRS-99] M. Schubert et al., MRS Internet J. Nitride Semicond. Res. 4, 11 (1999).

[Schubert-PRB-00] M. Schubert, T. E. Tiwald, and C. M. Herzinger, *Phys. Rev. B*, 62, 040002 (2000).

[Kasic-00] A. Kasic, M. Schubert, S. Einfeldt, and D. Hommel, unpublished.

[Gleize-99] J. Gleize et al., *Appl. Phys. Lett.* 74, 703 (1999).

[Davydov-97] V. Yu. Davydov et al., *J. Appl. Phys.* 82, 5097 (1997).

[Tripathy-99] S. Tripathy et al., *J. Appl. Phys.* 85, 8586 (1999).

[Barker-73] A. S. Barker, Jr. and M. Huggins, *Phys. Rev.* B7, 743 (1973).

[Perlin-96] P. Perlin et al., *Appl. Phys. Lett.* 68, 1114 (1996).

[Kim-97] K. Kim et al., *Phys. Rev. B* 56, 7363 (1997).